SYNTHESIS, CHARACTERIZATION, AND ANTIFUNGAL ACTIVITY OF SOME NOVEL TRANSITION MIXED LIGANDS METALS(II) COMPLEXES OF SUCCINATE AND PYRAZOLE DERIVATIVES

A.S.A. Albotani[1], H.F. Mohamedameen[1], K.S. Al-Nama[1*], S.M. Saied[2], M.Y. Saleh[3]

[1]University of Mosul, College of Science, Department of Chemistry, Mosul, Iraq
[2]University of Alnoor, College of Health and Medical Technologies, Nineveh, Mosul, Iraq
[3]University of Mosul, College of Education for pure Science, Department of Chemistry, Mosul Iraq
**e-mail: khnsaash.al-nama@uomosul.edu.iq*

Received 09.12.2025
Accepted 20.02.2026

Abstract: *The aim of this study was to synthesize new complexes and evaluate their effectiveness on some strains of Candida albicans. Miconazole was used as a positive antifungal control. One of the generated compounds exhibited good inhibitory activity against the tested fungi. The general formula of the synthesized compounds was K[M(SC)(PY)(H_2O)Cl], where M = Co(II), Ni(II), Cu(II), Zn(II), and Cd(II). These complexes were synthesized by the interaction of succinate (SC) or pyrazole (PY) crab ligands as mixed ligands with metal chlorides in ethanol media in a molar ratio of L^1:M:L^2 (1:1:1). The formation of the synthesized complexes was confirmed by Fourier Transform Infrared (FT-IR) and UV-Vis spectra, as well as ^{1}H and ^{13}C-NMR studies. Melting temperatures, molar conductivity, magnetic susceptibility, atomic absorption, CHN, and UV-visible studies were also carried out. The geometrical form of the complexes was suggested to be octahedral. Quantum chemical calculations of various quantum chemical descriptors such as FMOs were calculated using density functional theory (DFT).*
Keywords: *Antifungal activity, DFT, pyrazole, succinate, mixed ligands.*

1. Introduction

In contrast to typical complexes, mixed ligand complexes have at least two distinct ligand types bound to a single metal ion. The likelihood of the compound's predicted qualities changing is increased when one type of ligand is present. Mixed ligand synthesis and characterization have grown in significance. Many researchers are working in this field due to the increased interest in it [1-4]. Pyrazoles are an important class of compounds because of their biological and pharmacological activities [5]. Furthermore, fused pyrazole moieties exhibit a variety of intriguing features, including anti-hyperglycemic, analgesic, anti-inflammatory, anti-pyretic, anti-bacterial, and sedative-hypnotic effects [6,7]. Recently, certain pyrazoles have been shown to inhibit non-nucleoside HIV-1 reverse transcriptase [8, 9].

This study aims preparation, characterization and assessment the antifungal activity of Co^{+2}, Ni^{+2}, Cu^{+2}, Zn^{+2} and Cd^{+2} complexes. These are synthesized from 4-aminoantipyrine (PY) and succinate (SC) as mixed ligands. All synthesized complexes were characterized by FTIR, UV-Vis, ^{1}H-, and ^{13}C-NMR spectroscopy, CHN, and various physicochemical methods. Frontier molecular orbitals (FMOs) and various quantum chemical descriptors (QCDs) were calculated using density functional theory. Additionally, the synthesized compounds were evaluated against the fungus *Candida albicans.*

2. Experimental part

2.1. **Materials Employed:** All chemicals used were purchased from Sigma Aldrich and BDH.

2.2. Instrumentations. The measurements were carried out using an SMP10 Automatic Melting Point apparatus from the British company STUART. Infrared spectra of the synthesized compounds were recorded using an FTIR, a Bruker Alpha FTIR, in the range of 4000-400 cm^{-1}. DMSO-d_6 was used as the solvent in a Bruker Analytical 400 & 100 MHz spectrometer to record NMR spectra. Using quartz cells and DMF as the solvent, UV-vis spectral measurements were

performed with a PerkinElmer Lambda 365 spectrophotometer. A Sherwood Scientific MK1 device was used to measure the magnetic susceptibility of the compounds produced. The elemental microanalysis was recorded using Elementar Analysensysteme GmbH, CHNS. The molar conductivity of 10^{-3} M solutions of the compounds in DMSO was determined using a Jenway Model 4510 conductivity meter. An atomic absorption spectrometer (Analytik Jena) was also utilized.

2.3. Preparation of metal ion complexes. The preparation of the metal complexes was achieved through a stepwise procedure. Initially, SC (L^1) (0.118 g, 1 mmol) was dissolved in 10 ml of an aqueous KOH solution ($1x10^{-3}$ M). The basic solution was added carefully to a hot ethanolic medium (20 ml) containing 1 mmol of the respective hydrated metal chlorides: $CoCl_2 \cdot 6H_2O$ (0.237 g), $NiCl_2 \cdot 6H_2O$ (0.237 g), $CuCl_2 \cdot 2H_2O$ (0.17 g), $ZnCl_2$ (0.136 g), and $CdCl_2$ (0.183 g). The pH of the solution was adjusted to 9, and the change in color that accompanied this step suggested the onset of PY (L^2) (0.203 g, 1 mmol) in 15 ml of ethanol, which was introduced dropwise into the reaction mixture with continuous stirring at 80°C. After 3-4 h of reflux, solid products of different colors, depending on the metal precipitates, were filtered, washed repeatedly with hot distilled water followed by diethyl ether, recrystallized from ethanol, and dried at ambient temperature [10,11]. The overall synthetic pathway for the complexes is presented in Scheme 1.

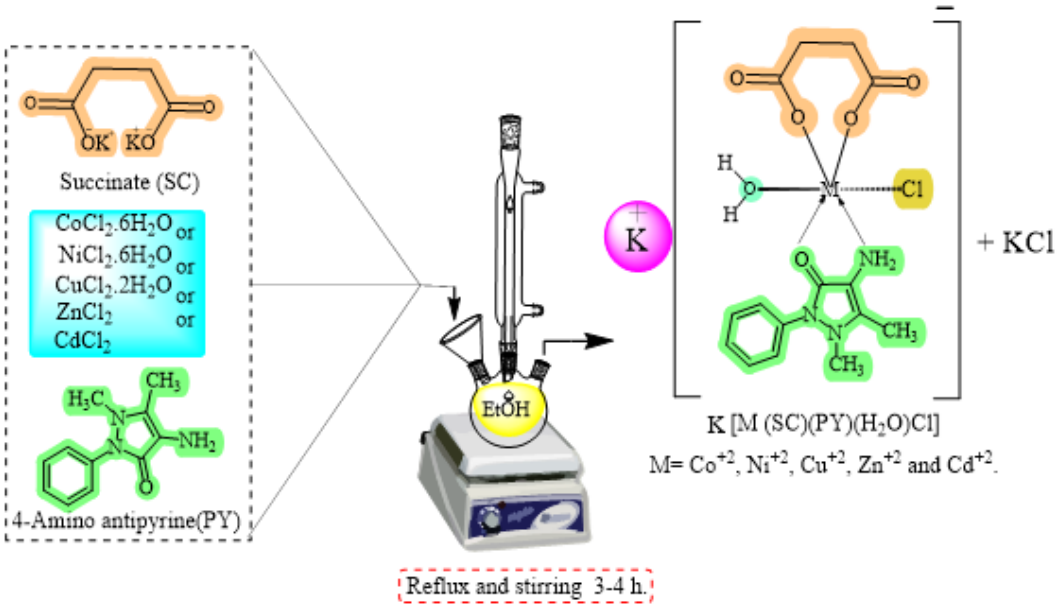

Scheme 1. Suggested structure of the synthesized complexes

2.4. Density Functional Theory (DFT). In the absence of X-ray crystallographic information, molecular modeling has become an important technique in the structural analysis of coordination complexes, as it provides additional structural insights and low-energy structures [11-13]. Through a study of DFT, the stability of a molecule can be thoroughly analyzed using various computational techniques and parameters. Discussing the stability of a molecule allows for the optimization of molecular geometries; a vibrational frequency analysis can be performed, calculating the binding energy, which provides insight into the stability of interactions, such as ligands with receptors. Thermodynamic stability can be assessed by calculating Gibbs free energy, and analyzing molecular orbitals and electron density can yield insights into the stability of a molecule. Additionally, reaction pathways and energy barriers can be evaluated by calculating activation energies for reactions. In general, DFT provides a full suite of tools for the study of molecular stability from energy, structural and electronic points of view, shedding light onto specific properties at various physical scales [5]. Theoretical explanations were obtained based on frontier molecular orbitals (FMOs) and other quantum chemical descriptors. Density Functional Theory (DFT) was performed for the optimized complexes using a program GW9 in Gaussian 16. It was used for all DFT/B3LYP calculations. Standard basis sets were 6-31G (++), d, and p for the investigated compounds.

2.5. Antifungal activity. *Candida albicans* was the fungus against which the complexes were

tested. Miconazole was used as a positive control for antifungal activity, and DMSO was used as a negative control. The fungal strains were grown in Petri plates using nutrient agar medium and PDA broth media. The chemical was soaked in filter paper discs that were 5 mm in diameter and 1 mm thick after being dissolved in a DMSO solvent with different concentrations (10 mg/ml and 20 mg/ml). After the discs were placed on the plates that had been seeded earlier, they were incubated at 37°C for 5-7 days for the fungal strain. The diameter of the inhibitory zone surrounding each disc was then measured [12, 13]. The inhibition zones of fungal growth caused by the synthesized compounds are listed in Table 5.

3. Results and discussion

3.1. Conductivity, stoichiometry, and CHN analysis. The compounds were prepared by reacting 4-aminoantipyrine (PY) and succinate (SC) with some metal chlorides of the first transition elements under suitable conditions to synthesize mixed-ligand complexes, as shown in Scheme 1. The complexes are almost perfectly soluble in DMF and DMSO at room temperature. Table 1 provides the analytical data and physicochemical characteristics of each product molecule. Several techniques were used, such as molar conductivity, where values ranged from 38 to 47 Ω^{-1} cm^2 mol^{-1}. Using the molar spectroscopic measurement approach, the chemical proportions of metal ion compounds formed in solution as a result of the interaction of metal ions with the bonds studied were determined [14]. At a molar ratio of ≈1, two linear regions of the molar ratio graph overlap, illustrating the formation of the complexes in a 1:1:1 ratio (L^1:M:L^2). The results of the C.H.N. analysis and the metal content in the complexes were in good agreement with the calculated values, as shown in Table 1.

The physical properties of the compounds, including conductivity measurements, coloration, melting points, and magnetic moments, have been thoroughly described. These characteristics have provided a deep understanding of the characteristics and molecular structures of the synthesized metal complexes.

Table 1. The CHN analysis, conductivity, and physical properties of synthesized compounds

Compound	Color	M.p. (°C)	Yield %	Elemental analysis (%) Found (calc)				ΛM (Ω^{-1} cm^2 mol^{-1})
				C	H	N	M	
Co(II)-complex	Peggy	168-170	87%	38.26 (38.61)	4.06 (3.90)	8.92 (8.77)	12.51 (12.37)	47
Ni(II)-complex	Green	189-191	79%	38.28 (38.08)	4.07 (3.95)	8.92 (8.70)	12.47 (12.35)	38
Cu(II)-complex	Green	124-126	70%	37.86 (37.70)	4.02 (3.85)	8.83 (8.66)	12.35 (12.26)	40
Zn(II)-complex	Yellow	157-159	77%	37.74 (37.52)	4.01 (3.80)	8.80 (8.68)	13.69 (12.48)	38
Cd(II)-complex	Brown	178-180	74%	34.36 (34.20)	4.65 (3.55)	8.01 (7.88)	21.44 (21.28)	39

3.2. FTIR Spectrum. The FT-IR spectrum of free succinic acid (SC) displayed clear bands for the two carbonyl groups of υ(-COOH) at 1695 cm^{-1}, together with a broad (O-H) stretching band at 3591 cm^{-1}. In the spectra of prepared complexes, these bands were no longer observed, indicating that the carboxylic groups lost their protons during complex formation. Instead, two new bands corresponding to the asymmetric and symmetric stretching vibrations of the carboxylate groups, υas(COO^-) and υs(COO^-), were observed. The calculated Δυ values (υas-υs) were higher than 200 cm^{-1}, indicating that each carboxylate group coordinates to the metal ions through a single atom [4, 5]. Therefore, both υ(COO^-) groups of (SC) oxygen act as monodentate donors in the prepared complexes. On the other hand, 4-amino antipyrine (PY) shows two bands of υ(NH_2) at 3432 and 3325 cm^{-1} and υ(C=O)

at 1675 cm^{-1}. These two bands appeared at lower frequencies upon complex formation, indicating their coordination with the central metal ion. In the complexes, υ(OH) for H_2O appears at 3332-3462 cm^{-1}. Furthermore, a new band attributed to the symmetric and asymmetric vibrations of water molecules appears at 802-849 cm^{-1}. Bands of the (M-O) and (M-N) groups appeared in the ranges of 518-558 cm^{-1} and 443-494 cm^{-1}, respectively, for all the complexes [15,16]. FTIR spectral data of the complexes are listed in Table 2, and Fig.1 illustrates some spectra of the synthesized complexes.

Table 2. FT-IR Spectra bands for the synthesized compounds

Compound	υ(O-H) SC, υ (H2O)	υ(NH_2) PY	υC=O (PY), (SC)	υCOO-asym (SC)	υCOO-sym(SC)	υH_2O	υM-O	υM-N
L^1= SC	(3591) SC	----	(1695) SC	----	----	----	----	----
L^2= PY	----	3432 3325	(1675) PY	----	----	----	----	----
Co(II)-complex	(3462) H_2O	3255 3138	(1626) PY	1569	1322	836	528	443
Ni(II)-complex	(3332) H_2O	3351 3221	(1652) PY	1569	1302	830	558	459
Cu(II)-complex	(3438) H_2O	3325 3264	(1643) PY	1533	1300	802	518	494
Zn(II)-complex	(3448) H_2O	3353 3243	(1633) PY	1593	1335	849	551	443
Cd(II)-complex	(3420) H_2O	3312 3205	(1650) PY	1589	1313	809	543	466

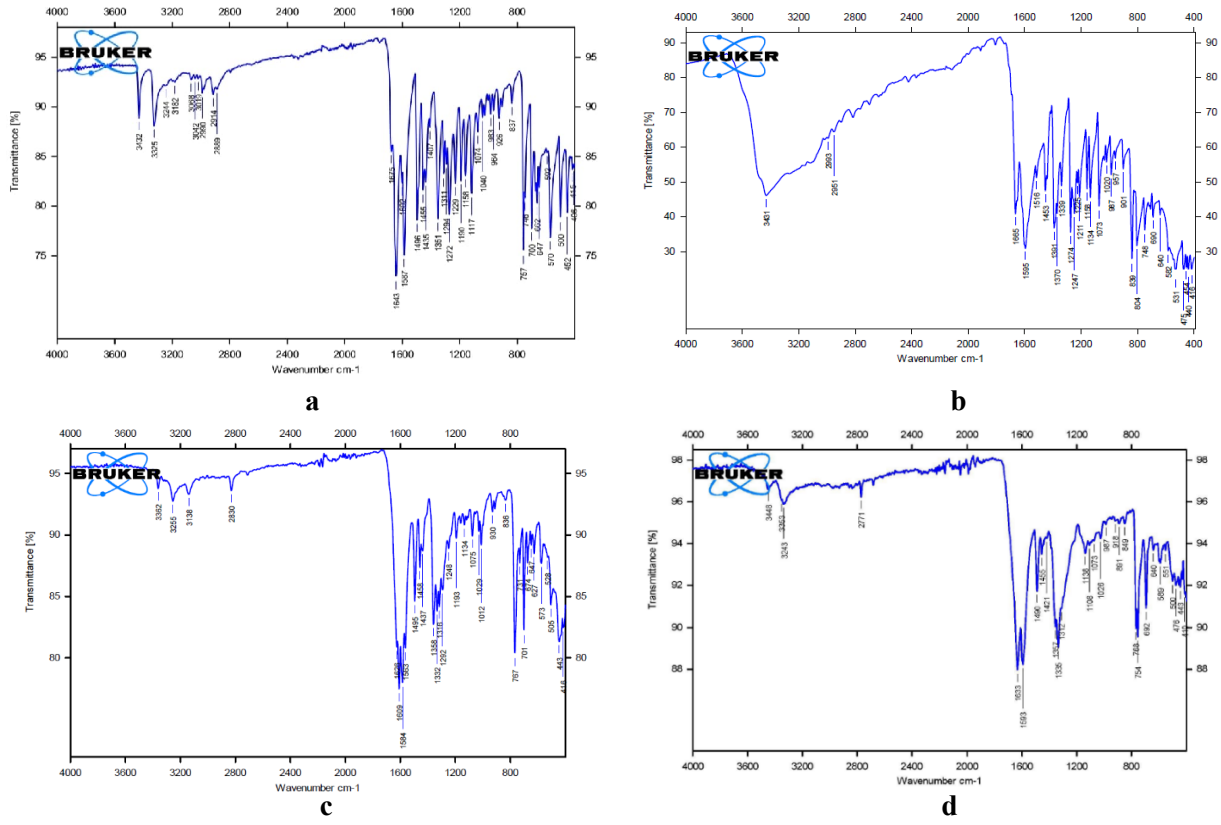

Fig. 1. FTIR spectra of (a) 4-aminoantipyrine, (b) succinic acid, (c) Co(II), and (d) Zn(II) complexes

3.3. ^{1}H- and ^{13}C-NMR Spectra of some synthesized complexes. The ^{1}H-NMR spectrum of free 4-aminoantipyrine (PY) recorded in DMSO-d_6 shows aromatic proton signals at 7.30-7.58 ppm, together with singlet signals assigned to the -NH_2 groups at 4.6 ppm, as well as resonances due to the methyl groups at 2.17 and 3.20 ppm. The free succinate (SC) co-ligand exhibits protons of a

singlet signal at 2.66 ppm. Meanwhile, the ^{13}C-NMR spectrum of free PY displays aromatic carbon signals in the range of 129.6-130.5 ppm, along with resonances assigned to the methyl carbons at 13.0 and 33.0 ppm, respectively, and the (CH=CH) of the pyrazole ring at 133.0 and 117.0 ppm, while the carbonyl is at 171.0 ppm. The free succinate (SC) co-ligand shows one carbon signal at 33.0 ppm and dicarboxylic carbons at 177.0 ppm [16, 17]. On the other hand, the synthesized complexes of Zn(II) and Cd(II) proton ^{1}H NMR spectra exhibited clear chemical shifts supporting the presence of different functional groups in the spectrum, such as the protons of the primary amine group bonded to the 4-aminoantipyrine group, which exhibited a singlet signal (NH_2, 2H) at 3.86 and 3.89 ppm, respectively [18, 19]. The chemical shifts in the 7.21-8.39 ppm and 7.00-8.5 ppm ranges of the multiplet signals (5H, aromatic) correspond to aromatic proton resonances. In addition, a signal appeared that was due to the protons of the coordinated water molecule alongside the deuterium water protons. The integrals for the protons in the spectra match the structural formula of the mixed ligand in the Zn(II) complex. While the ^{13}C NMR spectra were obtained, weak signals at 167.24, 161.67, 161.87, and 167.85 ppm were identified as the carbon atoms of the carbonyl of carboxylic and carbonyl amide groups, respectively, in the Zn(II) and Cd(II) complexes. Additionally, within the chemical shift range of 112.48-136.05 and 112.47-136.85 ppm, distinctive signals were observed for aromatic carbon atoms, respectively, providing significant structural data about the synthesized complexes. The number of carbon atom signals in the spectrum corresponds to the number of carbon atoms in the chemical formula of the prepared complexes. Fig. 2 illustrates the ^{1}H- and ^{13}C NMR spectra of the Zn(II) and Cd(II) synthesized complexes.

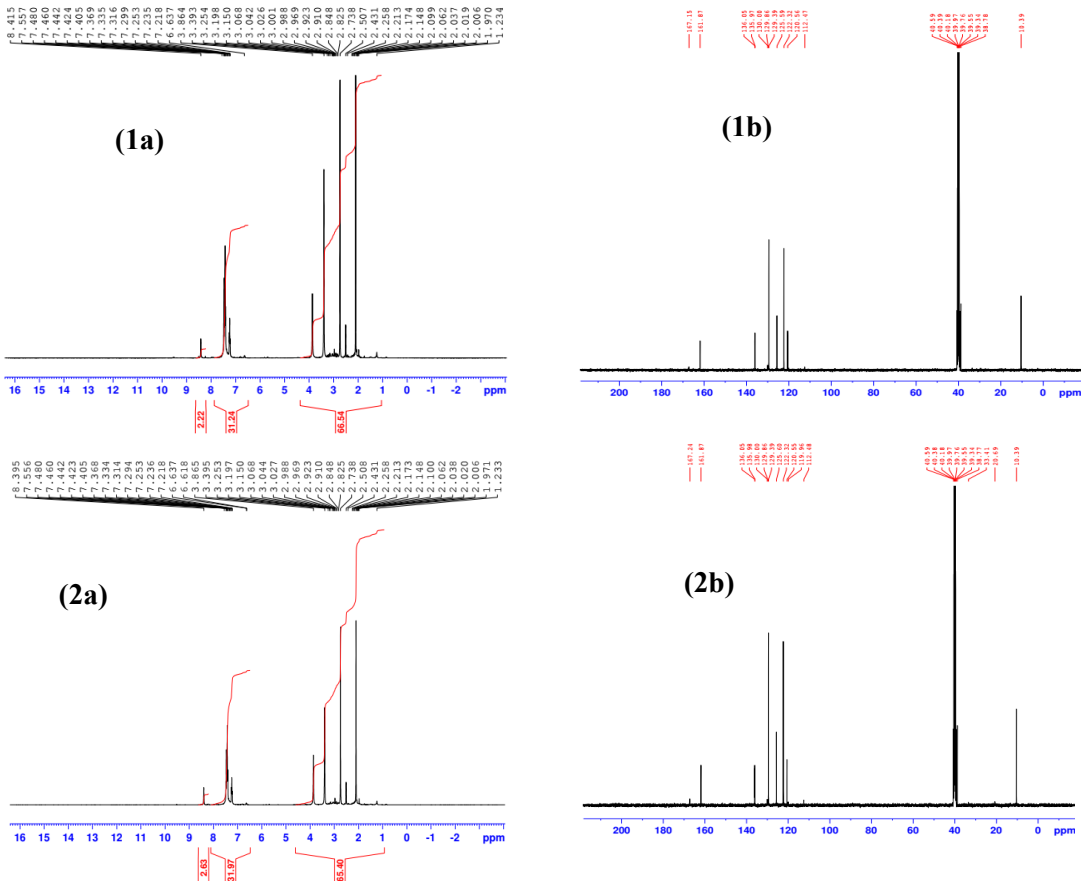

Fig. 2. (1a-2a)^{1}H- and (1b-2b) ^{13}C-NMR spectra of the synthesized Zn(II) and Cd(II) complexes

3.4. UV-Vis spectrum and magnetic studies. The UV-Vis spectra of the complexes revealed new absorption bands after coordination reflecting clear electronic changes in the ligands. Magnetic measurements supported the interpretation of their stereochemistry. For Co(II) complex bands at 14744, 18828, 29930, and 30233 cm^{-1} were attributed to the expected d-d transitions along with charge – transfer effects. The magnetic moment of 4.93 B.M. at room temperature is characteristic

of a high-spin d^7 system with octahedral geometry. The Ni(II) complex exhibited absorption at 11852, 14942, 24736, and 29018 cm^{-1} assigned to typical octahedral d-d transition with charge – transfere effects. Its magnetic moment 3.72 B.M., is consistent with a d^8 configuration in an octahedral field as seen in Table 3. In the case of the Cu(II) complex, two bands were observed at 14200, and 30225 cm^{-1} corresponding to the $^2E_1g \rightarrow {}^2T_2g$, transition and charge – transfer processes. The magnetic value of 1.74 B.M., confirmed the presence of a single unpaired electron in an octahedral environment. The Zn(II) and Cd(II) complexes exhibited ligand-to-metal charge-transfer bands at 28762, 30414, and 32978 cm^{-1} and 27821, 28326, and 33510, respectively. The absence of unpaired electrons is further supported by the octahedral geometries of the Zn(II) and Cd(II) complexes, which show no discernible magnetic moment [17, 19]. The unique coordination environments of the synthesized complexes are supported by this evidence. Table 3 provides a detailed description of the electronic spectra data and magnetic characteristics.

Table 3. Electronic spectral data of metal complexes, including ligands and magnetic moments

Compound	μ_{eff} (B.M)	Absorption (cm^{-1})	Assignment	Geometry
L^1 = SC	--	34162, 31219	$\pi \rightarrow \pi^*$, n $\rightarrow \pi^*$	--
L^2= PY	--	33916,31861	$\pi \rightarrow \pi^*$, n $\rightarrow \pi^*$	--
Co(II) complex	4.93	14744, 18828, 29930,30233	^4T_1g (F) $\rightarrow {}^4T_2g$(F), ^4T_1g (F)$\rightarrow {}^4A_2g$ (F), ^4T_1g (F)$\rightarrow {}^4T_2g$(P), C. T	Octahedral
Ni(II) complex	3.72	11852,14942, 24736, 29018	^3A_2g(F) $\rightarrow {}^3T_2g$(F), $^3A_2$ g (F) $\rightarrow {}^3T_1g$(P), A_2 g (F) $\rightarrow {}^3T_1g$(P), C. T	Octahedral
Cu(II) complex	1.74	14200, 30225	$^2E_1g \rightarrow {}^2T_2g$, C. T	Octahedral
Zn(II) complex	Dia	32978 ,30414, 28762	$\pi \rightarrow \pi^*$, n $\rightarrow \pi^*$, C. T	Octahedral
Cd(II) complex	Dia	33510, 28326, 27821	$\pi \rightarrow \pi^*$, n $\rightarrow \pi^*$, C. T	Octahedral

* C.T = Charge transition

3.5. Structure configuration of the complexes. Previously, Table 1 included the analytical data as well as the physical characteristics of the compounds. Each compound exhibits constant temperature stability and is insensitive to airborne moisture and oxygen. Excellent solubility in various solvents, such as DMSO, MeOH, acetone, and DMF, was evaluated for chelate complexes. There is an acceptable degree of agreement between the conclusions of the elemental analysis and the results obtained. Molar electrical conductivity, FT-IR spectroscopy, UV-Vis spectroscopy, NMR spectroscopy, and other analytical techniques were employed for the study. The analytical data and measurement findings of the complexes correspond well, demonstrating their accuracy. Particularly, based on the information in the previously mentioned Table 1, the molar ratio of the complexes Co(II), Ni(II), Cu(II), Zn(II), and Cd(II) was [1L:1M:1L], where the bidentate for each ligand (PY) and (SC) coordinates with metal ions through (N,O) and (COO-) atoms, respectively. FT-IR, molar conductivity, μeff (B.M.), and UV-Vis spectra suggest an octahedral shape for the investigated metal chelates K[M(SC)(PY)(H_2O)Cl], where M = Co^{+2}, Ni^{+2}, Cu^{+2}, Zn^{+2} and Cd^{+2}, complexes, as shown in Scheme 1.

3.6. Density functional theory (DFT) calculations. Density functional theory (DFT) simulations were used to examine frontier molecular orbitals (FMOs) in order to learn more about the stability, reactive characteristics, molecular interactions, and physicochemical aspects of the newly synthesized complexes [11-16]. In the study of kinetic stability, biological activity, polarizability, chemical reactivity, and a molecule's softness-hardness, HOMO-LUMO energies are recognized as an interesting area. The HOMO was the deepest electron-containing orbital and an electron donor. Indication of Nucleophilic or Electrophilic Attack So far, it is becoming apparent that the vulnerability of a molecule to attack by nucleophiles or electrophiles depends on its HOMO and LUMO orbitals, respectively [5, 17]. The EHOMO and ELUMO values of the complexes (1–5) are presented in Table 4. Both EHOMO and ELUMO are negative values, which means that the products

would be stable. The optimized geometrical structures and EHOMO/ELUMO values of chelates (1–5) are presented in Fig. 3.

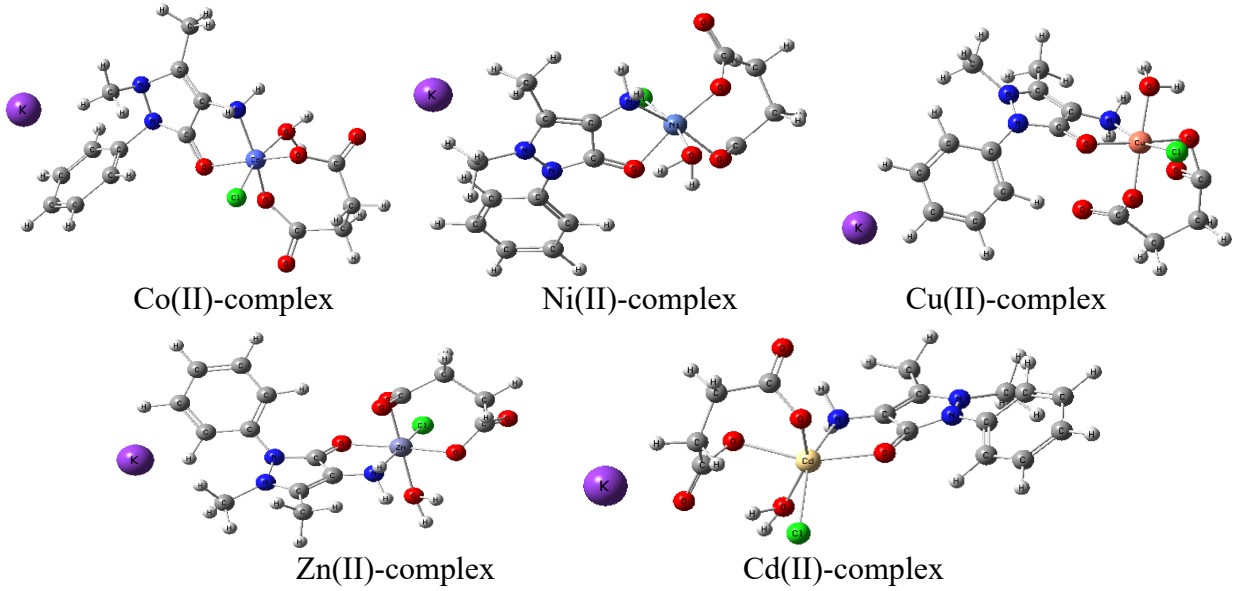

Fig. 3. The optimized structures of synthesized metal complexes (1-5)

The energies of HOMO and LUMO were calculated using the DFT/B3LYP method with a 6-311G+(d, p) basis set. These data were also employed to describe other QCDs, such as the chemical potential (μ), electronegativity (χ), global hardness (η), global softness (S), and the global electrophilicity index. The physical meaning of these QCDs has been well documented. [12, 15]. The optimized HOMO and LUMO orbitals of the synthesized metal complexes (1-5) are presented in Fig. 4.

The theory of minimal electrophilicity may be used to calculate the reactivities of both ligand and metal complexes. The concept of minimum electrophilicity (ω) claims that most stable moieties are those with the minimal electrophilicity [5], as is clearly seen in Table 4.

Table 4. Identified quantum chemistry characteristics of synthesized metal complexes (1-5)

Compound	E_{HOMO} (eV)	E_{LUMO} (eV)	ΔE (eV)	χ (eV)	η (eV)	σ $(eV)^{-1}$	–Pi (eV)	S $(eV)^{-1}$	ω (eV)	ΔN_{max} (eV)
Co(II)complex	-4.631	-1.867	2.765	4.631	1.867	1.382	3.248	0.723	1.357	4.631
Ni(II)complex	-7.650	-3.196	4.454	5.423	2.227	5.423	1.382	3.248	0.723	1.357
Cu(II)complex	-4.169	-3.028	1.141	3.599	0.571	1.753	3.599	0.876	11.349	6.308
Zn(II)complex	-5.037	-2.322	2.715	3.680	1.358	0.737	3.680	0.368	4.987	2.710
Cd(II)complex	-5.033	-3.802	1.231	4.418	0.616	1.625	4.418	0.812	15.85	7.177

*χ = -(ELUMO + EHOMO)/2, η = (ELUMO - EHOMO)/2, $\sigma = 1/\eta$, $Pi = -\chi$, $S = 1/2\eta$, $\omega = Pi^2/2\eta$, and $\Delta N_{max} = -Pi/\eta$

4. Antifungal activity. DMSO was used as a negative control, while miconazole was utilized for antifungal activity (positive control). The in vitro fungal activity results show that all of the metal complexes are more active than the ligands [20, 21]. The Ni^{+2} complex was found to be highly active at a concentration of 2 mg/ml. The Zn^{+2} complex was found to be more active in the second degree after Ni(II) compared to the other metal complexes. While the Co^{+2}, Cu^{+2}, and Cd^{+2} complexes showed slight activity. Table 5 displays the antifungal activity against *Candida albicans* by metal complexes.

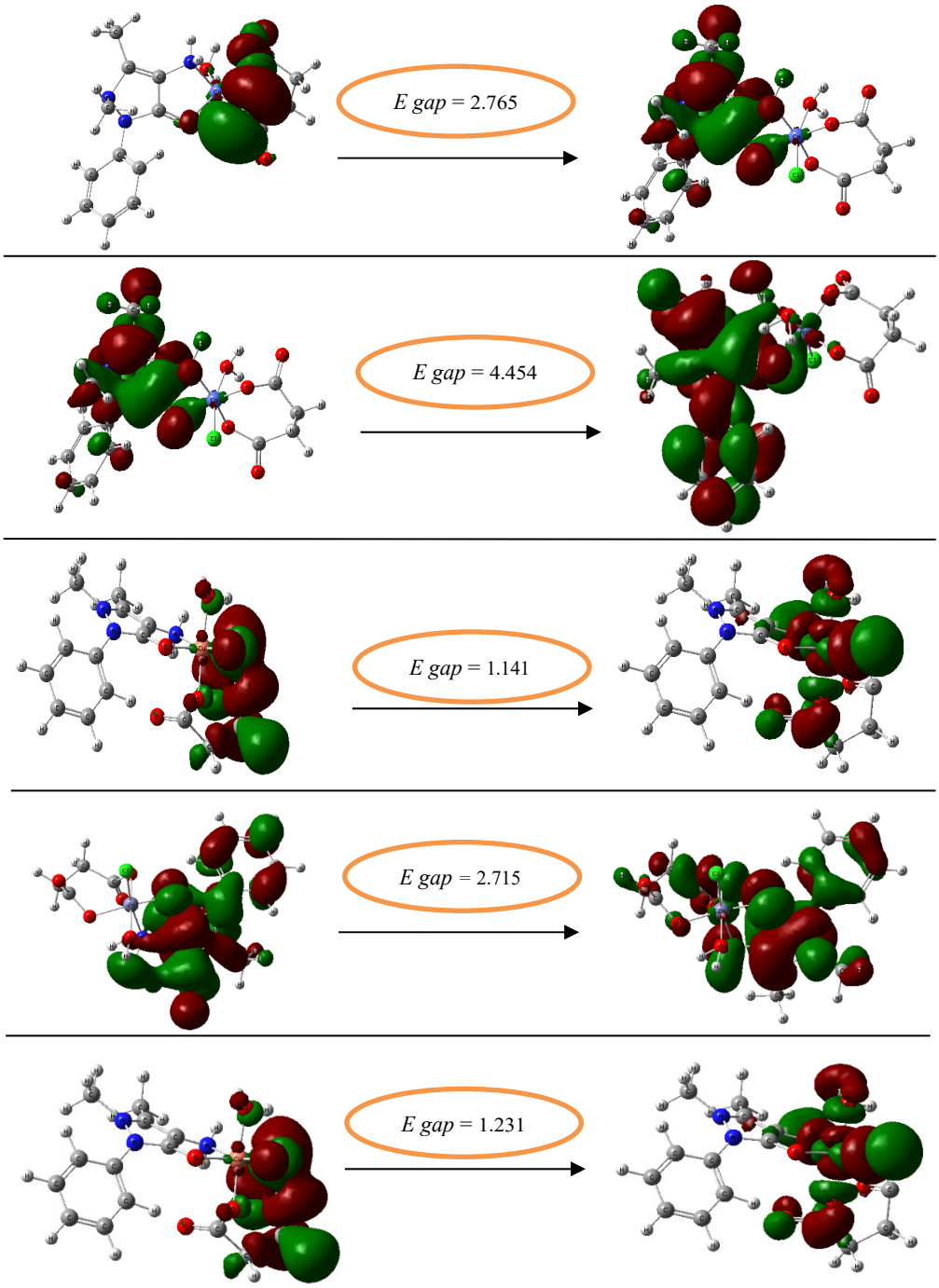

Fig. 4. HOMO and LUMO orbitals of the synthesized metal complexes (1-5)

Table 5. The inhibition zones of the synthesized compounds against the antifungal *Candida albicans.*

Compound	1mg/ml	2mg/ml
K[Co(SC)(PY)(H_2O)Cl]	2mm	6mm
K[Ni(SC)(PY)(H_2O)Cl]	6mm	11mm
K[Cu(SC)(PY)(H_2O)Cl]	2mm	4mm
K[Zn(SC)(PY)(H_2O)Cl]	4mm	7mm
K[Cd(SC)(PY)(H_2O)Cl]	2mm	4mm
Miconazole	16mm	18mm
DMSO	2mm	2mm

Conclusions

Mixed-ligand compounds containing Co^{2+}, Ni^{2+}, Cu^{2+}, Zn^{2+}, and Cd^{2+} ions were synthesized and subjected to spectroscopic analysis. Infrared spectra showed the coordination of the SC ligand through the oxygen of the dicarboxylic groups. On the other hand, the PY ligand needs to be coordinated in a bidentate form via coordinating through the nitrogen atom of the amine and oxygen atoms of carbonyl groups. Five metal complexes were synthesized in a 1:1:1 (L^1:M:L^2) molar ratio. Metal (II) ion complexes were characterized using physicochemical and spectroscopic methods, including (^{1}H, ^{13}C-NMR, UV-Vis, FT-IR spectroscopy, CHN analysis, magnetic moments, and conductivity measurements), confirming the proposed structures. Physicochemical characterization and analytical data demonstrate that the complexes exhibit octahedral geometry. Predicting the optimal geometries of the complexes and their frontier molecular orbitals using DFT and the B3LYP approach provided deeper insight into their molecular characteristics. According to antifungal activity, the Ni^{+2} complex showed higher antifungal activity than all other complexes.

Acknowledgments

The author expresses his sincere thanks to the Department of Chemistry, College of Sciences, University of Mosul, for their indispensable assistance throughout this research. Also, a deepest appreciation and a heartfelt thanks to Al-Noor University, of Mosul, Iraq, for their financial support (ANUI/2025/SCI22) in publishing this research.

References

1. Olliaro P., Wells T.N.C. The global portfolio of new antimalarial medicines under development. *Clin. Pharmacal. Ther*. 2009, **Vol. 85(6)**, p. 584-595. DOI: 10.1038/ clpt.2009.51
2. Jaouen G., Vessières A., Top S. Ferrocifen type anticancer drugs. *Chem. Soc. Rev,* 2015, **Vol. 44(24)**, p. 8802-8817. DOI: 10.1039/C5CS00486A
3. Ornelas C. Application of ferrocene and its derivatives in cancer research. *New J. Chem*. 2011, **Vol. 35(10)**, p. 1973-1985. DOI: 10.1039/C1NJ20172G
4. Al-Shaheen A.J., Al-Bergas A.F. Synthesis and identification of some complexes of 4-[N-(2, 4-dihydroxybenzylidene) imino] antipyrinyl with serine (L1) or with theronine (L2) ligands and evaluation of their bacteria activities. *J. Educ. Sci*, 2020, **Vol. 29(4)**, p. 42-61. DOI: 10.33899/edusj.2020.126837.1058
5. Fatima A.W., Sahbaa A.A. Synthesis, DFT, docking analysis, and antibacterial assessment of complexes derived from metal (II)with the isatin- coumarin ligand. *Bull. Chem. Soc. Ethiop*, 2025, **Vol. 39(12)**, p. 2371-2388. DOI: 10.4314/bcse.v39i12.1
6. Metzler-Nolte N., Salmain M., Stepnicka P. The bioorganometallic chemistry of ferrocene. *Ferrocenes: ligands, materials and biomolecules*, 2008, **Vol. 5**, p. 499. DOI:10.1002/9780470985663
7. Abbaoui Z., Khibech O., Oulous A., Karci H., Dündar M., Özdemir İ., Touzani R. In silico and in vitro evaluation of N-heterocyclic derivatives as antimicrobials: ADMET analysis, SAR, and molecular docking. *In Silico Pharmacol*, 2025, **Vol. 3(3)**, p. 163. DOI: 10.1007/s40203-025-00445-y
8. Al-burgus A.F., Ali A.F., Al-abbasy O.Y. New spiro-heterocyclic coumarin derivatives as antibacterial agents: design, synthesis and molecular docking. *Chimica Techno Acta*, 2024, **Vol. 11(3)**, p. 11-13. http://elar.urfu.ru/handle/10995/138715
9. Abbaoui Z., Khibech O., Karci H., Dündar M., Özdemir İ., Gürbüz N., Alghibiwi H. Synthesis, characterization, and anticancer evaluation of N-Heterocyclic entities: ADME profiling and In Silico predictions. *Toxicol. Rep.*, 2025, **Vol. 16(10)**, p. 102-184. DOI: 10.1016/j.toxrep.2025.102184
10. Prabakaran A., Maheswari C.U., Issaoui N., Al-Dossary O.M., Rajamani T., Gnanasambandan T., Manikandan A. Computational insight into the spectroscopic and molecular docking analysis

of estrogen receptor with ligand 2, 3-dimethyl-N [2-(hydroxy) benzylidene] aniline. *J. King Saud. Univ. Sci*. 2024, **Vol. 36(10),** 103196. DOI: 10.1016/j.jksus.2024.103196

11. Mustafa N.A., Ahmed S.A. Design, synthesis, characterization, DFT, molecular docking, and in vitro screening of metal chelates incorporating Schiff base. *Bull. Chem. Soc. Ethiop*, 2024, Vol. 38(6), p. 1625-1638. DOI: 10.4314/bcse.v38i6.10
12. AL-Nama K.S., Saeed I.A., Mohammed A.F. Synthesis, characterization, DFT, molecular docking, and in vitro screening of metal chelates incorporating Schiff base. *Bull. Chem. Soc. Ethiop*, 2025, **Vol. 39(4)**, p. 687-701. DOI:10.4314/bcse.v39i4.7
13. Al-Obedi A.D., Al-Nama K.S. Computational binding studies and bioactivity evaluation for certain Schiff base metal-complexes transformed from ciprofloxacin. *Chemical Problems,* 2025, **Vol. 23(3)**, p. 449-461. DOI: 10.32737/2221-8688-2025-3-449-461
14. Kiss L., Ameen H.M., Lemli B., Kunsági-Máté S. Determination of Solubility of 4-(2-Hydroxyethyl)-1-piperazineethanesulfonic Acid and its Sodium Salt in Acetonitrile and Voltammetric Investigation of Sulphonamide Drugs in Different Solvents in Their Absence and Presence. *Journal of Solution Chemistry*. 2021, **Vol. 50(1)**, p. 147-159. DOI:10.1007/s10953-020-01047-2
15. Ahmed S.A. Nano-Schiff base Ligand: Synthesis, Characterization, DFT, and Antibacterial Evaluation of Some Complexes Derived From 4-(-4-methoxybenzylidene) amino)-Antipyrinyl with Glycine amino acid ligand. In *Journal of Physics: Conference Series*, IOP Publishing. 2021, **Vol. 1999(1)**, 012003.
16. Wagaa A., Ali F., Ahmed S.A. Metal Pharmacologically Active Agents: Mode of New Tridentate Glycine amino acid with diketone (Benzil) and 4-Amino antipyrine Complexes. *Egypt. J. Chem*. 2022, **Vol. 65(5)**, p. 59-67. DOI:10.21608/EJCHEM.2021.70792.3560
17. Qorri I., Haily E.M., Abbaoui Z., Boulouiz A., Touzani R., Karci H., Ozdomir I. Synthesis, characterization, and dual applications of novel pyrazole-based ligands and their copper (II) complexes: anticancer, antimicrobial, and catalytic properties. *Discov. chem*, 2025, **Vol. 2(1)**, p. 3-55. DOI: 10.1007/s44371-025-00443-1
18. Ridal Z., Abbaoui Z., Elmsellem H., Aouniti A., Yousfi E.B., El Kodadi M., Hammouti B. Multifaceted Applications of Pyrazole-Based Tetradentate Ligand Coordinated with Transition Metals (Fe, Zn, Co, Cu): Synthesis, Characterization, Catalysis, Antimicrobial Activity, ADMET, and Molecular Docking Insights. *AJSE*, 2026, **Vol. 6(2)**, p. 149-172. DOI: 10.17509/ajse.v6i1.89885
19. Mohammed A.F., Saeed I.A., AL-Nama K.S. Synthesis, diagnosis as well as biological activity studies of some metal ion complexes of Schiff Bases Derived from 4-aminoantipyrine. *Baghdad Sci. J.* 2025, **Vol. 2(2)**, p. 2. DOI: 10.21123/ bsj.2024.9204
20. Al-Agwan N.N., AL-nama K.S., Abdulrahman S.H. Design, synthesis, antioxidant potential, antibacterial and molecular docking insights of Schiff base complexes. *Bull. Chem. Soc. Ethiop,* 2025, **Vol. 39(11)**, p. 2157-2171. DOI: 10.4314/bcse.v39i11.6
21. Wodi T.C., Festus C. Multifaceted Investigations of Mixed-Ligand Metal (II) Complexes: Synthesis, Characterization, DFT, and Biological Studies. *Sci. Innovations,* 2025, **Vol. 6(3)**, p. 1-14. DOI: 10.63561/fnas-jsi.v6i3.945